available at www.sciencedirect.com

ScienceDirect

journal homepage: www.ejconline.com

Targeting α7-nicotinic receptor for the treatment of pleural mesothelioma

Alessia Catassi[a,b], Laura Paleari[a], Denis Servent[c], Fausto Sessa[d,e], Lorenzo Dominioni[b], Emanuela Ognio[f], Michele Cilli[f], Paola Vacca[g,h], Mariacristina Mingari[g,h], Giovanni Gaudino[i], Pietro Bertino[i], Massimo Paolucci[i,j], Andrea Calcaterra[j], Alfredo Cesario[k,l], Pierluigi Granone[k], Roberta Costa[m], Monica Ciarlo[a], Angela Alama[a], Patrizia Russo[a,]*

[a]*Lung Cancer Unit, National Cancer Research Institute, 16032 Genoa, Italy*
[b]*Center for Thoracic Surgery, University of Insubria, 21100 Varese, Italy*
[c]*CEA, iBiTecS, Service d'Ingénierie Moleculaire des Protéines (SIMOPRO), Gif sur Yvette, F-91191, France*
[d]*Pathology Unit, University of Insubria, 21100 Varese, Italy*
[e]*Pathology Unit, Multimedica spa, 20100 Milan, Italy*
[f]*Animal Models Unit, National Cancer Institute, 16132 Genoa, Italy*
[g]*Immunology Section, National Cancer Research Institute, 16132 Genoa, Italy*
[h]*DIMES - Department of Experimental Medicine, University of Genova, 16132 Genoa, Italy*
[i]*DISCAFF University of Piemonte Orientale "A. Avogadro", Novara, Italy*
[j]*Radiology Unit, Gallarate Hospital, 21013 Gallarate (Varese), Italy*
[k]*Surgical Pathology Unit, Catholic University, Rome, 00168, Italy*
[l]*IRCCS 'San Raffaele', 00163 Rome, Italy*
[m]*Cardio-Thoracic Surgery Unit, Alessandria Hospital,15100 Alessandria, Italy*

ARTICLE INFO

Article history:
Received 27 March 2008
Received in revised form
16 June 2008
Accepted 30 June 2008
Available online 20 August 2008

Keywords:
α7-Nicotinic receptor
Mesothelioma
Apoptosis
Survivin
Antitumour activity

ABSTRACT

Human malignant pleural mesothelioma (MPM) is a dreadful disease and there is still no standard therapy available for a consistent therapeutic approach. This research is aimed at the evaluation of the potential therapeutic effect of a specific nicotinic receptor (nAChR) antagonist, namely α-Cobratoxin (α-CbT). Its effectiveness was tested in mesothelioma cell lines and in primary mesothelioma cells *in vitro*, as well as *in vivo*, in orthotopically xenotransplanted NOD/SCID mice. Cells showed α7-nAChR expression and their growth was significantly inhibited by α-CbT. Severe induction of apoptosis was observed after exposure to α-CbT [$IC_{80\text{-}90}$]. Apoptosis was characterised by: change in mitochondrial potential, caspase-3 cleavage, down-regulation of mRNA and protein for survivin, XIAP, IAP1, IAP2 and Bcl-XL, inhibition by caspase-3 inhibitor. *In vivo*, the α-CbT acute LD_{50} was 0.15 mg/kg. The LD_{100} [0.24 mg/kg] induced fatal respiratory failure and massive kidney necrosis. Phase II experiments with 0.12 ng/kg α-CbT (1/1000 of LD_{10}) were done in 53 xenotransplanted mice, inhibiting tumour development as confirmed by chest X-ray examinations, autopsy and microscopical findings. The growth of human proliferating T lymphocytes and of mesothelial cells in primary culture was not affected by α-CbT. Non-immunogenic derivatives of the α-CbT molecule need to be developed for possible human use.

* *Corresponding author*: Tel.: +39 0105737572; fax: +39 0105737571.
E-mail address: patrizia.russo@istge.it (P. Russo).
0959-8049/$ - see front matter
doi:10.1016/j.ejca.2008.06.045

1. Introduction

The respiratory epithelium in lung tissue expresses cholinergic enzymes regulating the levels of free acetylcholine (ACh), the vesicular ACh transporter, the choline high-affinity transporter, and shows functional cholinergic receptors (AChR).[1–3] The finding that nAChR are functionally present in human lung airway epithelial cells.[4–9] was followed by the observation of their expression in lung carcinoma (SCLC and NSCLC) or mesothelioma. In these cells, the cholinergic system forms part of an autocrine-proliferative network that facilitates cell growth.[9–12] Recently, it was shown that between NSCLC from smokers and nonsmokers, different nAChR subunit gene expression patterns are expressed, and a 65-gene expression signature was associated with non-smoking α77-nAChR expression.[13] Most recently, we have unambiguously demonstrated the presence of specific α7-nAChR, at the mRNA and protein levels, in human mesothelioma as well as in unaffected mesothelial cells.[12] In mesothelioma cells, in the presence of 30 mM KCl, nicotine binds to α7-nAChR and triggers an initial cytosolic influx of sodium that creates membrane depolarisation via entry of Ca^{2+} into the cytosol through the voltage-gated calcium channels. Almost immediately, as the level of MEKK-1 increases, MAPK are activated together with an increment of the level of phosphorylated p90RSK. Moreover, as a consequence of MEKK-1 increase, NF-κB complexes are activated, and cells enter the S phase of the cell cycle, increasing the rate of DNA synthesis followed by proliferation. In this process, p53 is not affected. As reported with A549 lung adenocarcinoma and MSTO-211H mesothelioma cell lines, nicotine strongly promotes phosphorylation of Bad Serine[112] and induces cell survival and proliferation.[1,12] On the contrary, D-tubocurarine (nAChR antagonist) inhibits mesothelioma cell growth.[12] Thus, D-tubocurarine leads MSTO-211H cells to accumulate in the G_0-G_1 and sub-G_0-G_1 fraction inducing $p21^{waf-1}$ p53-independently. D-tubocurarine reduces the levels of phospho-ERK, does not affect the expression of phosphorylated p90RSK and NFκB activity and, more importantly, does not activate phosphorylation of Bad Serine[112]. Consequently, the level of total Bad Serine increases and the process of apoptosis is triggered. These experiments imply that nAChR antagonists might interfere with the survival pathway mediated by α7-nAChR.

Various animal venom toxin antagonists of AChR [such as α-bungarotoxin (BGT) from the Bungarus multicinctus snake and conotoxins, purified from the venom of Conus marine snails] have previously been used as molecular tools for the characterisation of neuronal and non-neuronal nAChR in lung cancer and mesothelioma.[12] However, to our best knowledge, a direct cytotoxic effect of venom components against cancer cells has never been investigated and demonstrated. Several previous reports, not including any mechanistic aspects,[14,15] described some anticancer activity associated with snake venom.

We recently reported,[16,17] some data obtained in NSCLC regarding cell growth inhibition both *in vitro* and in a nude mice model (intraperitoneal or orthotopically transplanted) using one of the most powerful antagonists of the α7-nAChR, namely α-CbT. α-CbT is a member of the long α-neurotoxins (α-NTs) family obtained from the venom of Naja kaouthia. Herein, we address and report the causal relationships between α7-nAChR inhibition by α-CbT and cancer cell growth inhibition, both in mesothelioma cell culture and in orthotopically transplanted mice.

2. Materials and methods

2.1. Cell cultures and drugs

IST-MES2 and MPP89 cell lines, obtained by our Institutional Cell Repository (Genoa, Italy) and characterised by Orengo et al.[18] were grown in RPMI 1640 with 20% FBS (Gibco BRL, Grand Island, NY).

Primary mesothelioma cells were obtained by enzymatic digestion of fresh human surgical biopsies, as previously described.[12] Cryopreserved unaffected mesothelial cells (Mes1 and Mes2), obtained from two patients who underwent thoracotomy for non neoplastic diseases and previously characterised,[12] were cultured. Mesothelial cells were grown as primary cultures on fibronectin-coated culture flasks in RPMI 1640 supplemented with 20% heat-inactivated FBS (Life Technologies, Inc., Gaithersburg, Germany), epidermal growth factor (20 ng/ml), hydrocortisone (1 μM), insulin (10 μg/ml), transferrin (5 μg/ml), and (50 μg/ml) gentamicin (Life Technologies, Inc.) at 37 °C in a humidified 5% CO_2 atmosphere. Fresh complete medium was replaced every 2–3 days until cells were confluent. Upon confluence the cells were lifted by 1× trypsin-EDTA (Life Technologies, Inc.) and subcultured at a 1:2 dilution. The cells were identified as mesothelial cells by immunocytochemical staining with antikeratin antibodies (Dako, Glostrup, Denmark). The third and the fourth passage confluent cultures were used for cell growth.

α-Cobratoxin was purified from the Naja kaouthia venom as previously described.[19] The lyophilised powder was resuspended in PBS buffer + 0.1% BSA in order to reach the appropriate concentrations. The powder is stable for several months when stored at –20 °C and the dilution solutions for several weeks when stored at 4 °C. We used, in all experiments, natural α-CbT purified at 97% by HPLC.

2.2. Transfection of human MPP89 cells and evaluation of cytotoxicity

siRNA-7 was designed and custom synthesised by OriGene Technologies (Rockville, MD, USA). The target sequences for the human α7-nAChR mRNA (NM_000746) gene was 5′-GGACAGAUCACUAUUUACA-3′. For transfection with siRNA, we followed the standard protocol described in detail elsewhere by Arredondo et al.[36] Briefly, MPP89 cells were seeded at a density of 5×10^4 cells per well of a 24-well plate and incubated for 16–24 h to achieve 70% confluence. To each well, increasing concentrations of siRNA duplex in the transfection solution with the TransIT-TKO transfection reagent (Mirus, Madison, WI, USA) were added, and the transfection was continued for 16 h at 37 °C in a humid, 5% CO_2 incubator. On the next day, the transfection medium was replaced by RPMI 1640 and the cells were incubated for 72 h to achieve maximum inhibition of the receptor protein expression, as

experimentally determined by Western blot at different time points after transfection. The clone that did not express α7-nAChR protein was used in MTS experiments (cytotoxicity). The MTS assay was performed as previously described.[20] Cells were exposed to different concentrations of α-CbT for 72 h (continuous treatment).

2.3. Clonogenic assay in semisolid medium and apoptosis detection

Clonogenic assay in semisolid medium and apoptosis detection (Annexin V-PI staining, Internucleosomal DNA Fragmentation, DAPI staining) were performed as described previously.[12] For the Annexin V-PI assay, cells were treated for 30 h at 1.0 μM. Cells were washed in phosphate-buffered saline (PBS) and resuspended in 100 μL binding buffer containing Annexin V (Roche Diagnostic, Indianapolis, IN). Cells were analysed by flow cytometry after the addition of propidium iodide (PI). For inter-nucleosomal DNA fragmentation, adherent and detached cells were harvested, washed and lysed with 50 mM/L Tris, pH 7.5, 10 mM/L EDTA, 0.5% Triton-X-100, and 0.5 mg/mL proteinase K for 2 h at 50 °C. Samples were then extracted twice with phenol/chloroform/isoamyl alcohol and precipitated with ethanol. The pellet was resuspended in Tris-EDTA and 10-μg/mL ribonuclease A and the DNA was separated on a 2% agarose gel. Cells were treated with α-CbT for different time intervals. To detect the role of caspase-3, the caspase-3 inhibitor (zDEVD) at 20 μM was incubated for 30 min prior to cell treatment with α-CbT 1.0 μM for 30 h. For the DAPI assay, cells were washed twice in a chamber slide system (Nalge Nunc International, Naperville, IL) with PBS to remove non-adherent cells and were fixed with 4% formaldehyde in PBS for 30 min at room temperature. After washing with PBS twice, the cells were stained with DAPI (Sigma-Aldrich (working dilution, 1/1000) at 37 °C for 30 min and were observed by fluorescence microscopy.

2.4. Western Blot Analysis and RT-PCR

Western blot analysis and RT-PCR was evaluated as described previously.[12] Survivin was obtained from Novus Biologicals (Littleton, UK), caspase-3, XIAP, IAP1, IAP2 and BCL-XL from Abcam Ltd. (Cambridge, UK). The RT-PCR kit was obtained from Qiagen (Milan, Italy). After reverse transcription, the cDNA product was amplified by PCR with Taq DNA polymerase using standard protocols. The amplified products (10 μl) were separated on 2% agarose gels, stained with ethidium bromide and photographed using ultraviolet illumination. The 5′ forward and 3′ reverse complement PCR primers for amplification of survivin were CTGATTTGGCCCAGTGTTTT and TCATCTGACGTCCAGTTTCG, respectively. For cIAP2, PCR primers were ACATTTCCCCAGCTGCCCATTC and CTCCTGCTCCGTCTGCTCCTCT. For cIAP1, PCR primers were CCAGCCTGCCCTCAAACCCTCT and GGGTCATCTCCGGGTTCCCAAC. For XIAP, PCR primers were CGCGAGCGGGGTTTCTCTACAC and ACCAGGCACGGTCACAGGGTTC. For BCL-XL, PCR primers were AGAGAACAGGACTGAGGCCC and TCAAAGCTCTGATATGCTGTCCC. For glyceraldehyde-3-phosphate dehydrogenase (GAPDH), PCR primers were CCATCACCATCTTCCAGGAG and CCTGCTCACCACCTTCTTG. For ββ-actin, PCR primers were GTGGGGCGCCCCAGGCACCA and –CTCCTTAAGTCACGCACGATTTC.

For protein analysis, total cellular lysates were separated on a 12% (w/v) SDS-polyacrylamide gel and transferred to nitrocellulose using standard protocols. The filters were blocked in PBS with 5% skimmed milk and incubated overnight with primary specific antibodies. The filters were then incubated with the secondary peroxidase-linked whole antibodies (Amersham Biosciences Europe GmbH, Freiburg, Germany). Bound antibodies were detected using the enhanced chemiluminescence Western blotting detection system (Amersham Biosciences Europe).

2.5. Mitochondrial membrane potential assay

Mitochondrial membrane potential assay was measured with JC-1 (5, 5′, 6, 6′-tetrachloro-1, 1′, 3, 3′ tetraethylbenzimidazolylcarbocyanine iodide/chloride) detection kit (Stratagene La Jolla, CA) according to the manufacturer's instructions. JC-1 is able to enter mitochondria selectively, which appears green at low concentrations or at low membrane potential as a monomer. However, at high concentrations, mitochondria show as red fluorescent aggregates. JC-1 is sensitive to mitochondrial membrane potential and the changes in the ratio between green and red fluorescence can provide information of the mitochondrial membrane potential. After the treated cells were loaded with JC-1 1.0 μM/L for 10 min at 37 °C, the fluorescent dye was excited at 490 nm, and the fluorescence intensities of both monomer and aggregated molecules were recorded at 590 nm under a confocal scanning laser microscopy. For fluorescence ratio detection, 100 μl of the IST-MES2 stained cell suspension were transferred into each of three wells of a black 96-well plate. Red (585/590 nm) and green (510/527 nm) fluorescence were measured using a fluorescence plate reader. The ratio of red-to-green fluorescence is decreased in dead cells and cells undergoing apoptosis, compared to healthy non-apoptotic cells.

2.6. Animals and animal care

NOD/SCID mice (NOD.CB17-Prkdc$^{NOD/SCID}$/J) were born and housed in specific filter-capped cages, were kept in pathogen-free conditions and maintained in the facilities within the animal resources centre at the National Cancer Institute of Genoa in accordance with the recommendations, regulations and standards approved by the Federation of European Laboratory Animal Science Association. The mice were used in accordance with institutional guidelines when they were 8 weeks old and employed for both tumour maintenance and chemotherapy testing.

All the procedures involving animal care and treatment were conducted as stipulated in Italian National Guidelines (D.L. No. 116 G.U., suppl. 40, 18.2.1992, circolare No. 8, G.U. luglio 1994) and in the appropriate European Directives (EEC Council Directive 86/609, 1.12.1987), adhering to the Guide for the Care and Use of Laboratory Animals (United States National Research Council, 1996) and according to an approved protocol reviewed by the National Cancer's Institutional Animal Care and Use Committee (Genoa, 15 November 2004, n. of reference 149).

2.7. *In vivo orthotopical grafting of human mesothelioma cells*

In vivo NOD/SCID mice xenografts were obtained by grafting mesothelioma cells into the pleural space of 8-week-old female/male NOD/SCID mice. 100% reproducible tumour developments were obtained in each experiment. For ethical reasons, each animal underwent euthanasia (in a CO_2 atmosphere) after a 20% weight loss from the time of the tumour graft. An orthotopical model for mesothelioma was established by instilling IST-MES2, MPP89, MPP89-Luc, GMC1 or RC1 cells into the right pleural space of NOD/SCID mice. Cells were harvested for implantation at 70–80% confluence using 1 mM EDTA (Boehringer Mannheim, Mannheim, Germany) in PBS. The cells were washed in RPMI 1640 and resuspended to a final concentration of 5.0×10^6 cells/ml in RPMI 1640 containing 0.1% BSA (Boehringer Mannheim, Mannheim, Germany). To perform intrapleural instillation, mice were anaesthetised with an intraperitoneal injection of ketamin (100 mg/kg) and xylazine (10 mg/kg). After making a 5- to 10-mm incision through the skin on the right chest, a right anterolateral thoracotomy was performed in the fourth intercostal space, followed by instillation of 5×10^6 cells suspended in 100 μl PBS. The thorax was then closed by one pericostal suture and the skin reapproximated with an autoclip (MikRon Precision, Inc, Gardena, CA). Treatment started after 48 h, in order to allow recovery after surgery. Experiments were done with different treatment protocols, as detailed below.

2.8. *X-ray examination, necropsy, tissue preparation, haematoxylin and eosin (H&E) staining and immunohistochemistry*

Two months after cancer cell grafting, the mice underwent chest x-ray examination, under anaesthesia, using a Siemens Mammomat 3000 Nova, Kv 25 max 6.3 Film Kodak Min-R, and were then sacrificed with a lethal dose of sodium pentobarbital (100 mg/kg body weight). At autopsy, after thoraco-laparotomy, the thoracic cavity and the peritoneum were inspected for evidence of tumours. Visible tumour deposits were collected and the thoracic organs were then removed 'en bloc', including all the lymph nodes and tumours. After dissection and removal, the organs and the tumour masses were washed in cold PBS and weighed. For H&E staining procedures, one part of the tumour was fixed in formalin and embedded in paraffin, and another part was embedded in OCT compound (Miles, Inc., Elkhart, IN), rapidly frozen in liquid nitrogen, and stored at –80 °C. IHC determination of Calretinin was performed as described previously.[21]

2.9. *Evaluation of α-CbT toxicity*

The acute (5 days) i.v. LD_{10}, LD_{50} and LD_{90} of α-CbT were calculated treating 50 NOD/SCID mice of both sexes (20 females and 30 males) with different concentrations of α-CbT (from 0.004 to 0.20 mg/kg). LD_{10}, LD_{50} and LD_{90} were calculated using a log probit scale. Autopsy was performed in all animals. The liver, kidney, lung, brain, spleen and heart were removed and weighed. Tissues for microscopic examination were fixed and preserved in 10% neutral-buffered formalin, processed, embedded in paraffin, sectioned to a thickness of 4 to 6 μm, and stained with H&E. A complete histopathologic examination was performed. Blood samples were collected from the heart for haematology [in micro-collection tubes containing potassium EDTA (Sarstedt, Inc., Nümbrecht, Germany)] and clinical chemistry analyses (in tubes devoid of anticoagulant, allowed to clot at room temperature for serum separation). Erythrocyte, platelet, PMN and haemoglobin concentrations were determined using a Serono-Baker System 9000® haematology analyser (Serono-Baker Diagnostics, Allentown, PA). Clinical chemistry variables were measured using a Hitachi 704 chemistry analyser (Boehringer Mannheim, Indianapolis, IN) and commercially available reagents. To investigate the α-CbT effectiveness in the progressive tumour phase, mice xenografts obtained by grafting MPP89-Luc cells into the pleural space of 8-week-old female/male NOD/SCID mice (10 per group, the experiment was repeated twice) were treated at 14 days.

2.10. *Liver enzymes*

Serum levels of aspartate aminotransferase (AST), alkaline phosphatase (ALP), glutamic pyruvic transaminase (GPT) and γγglutamyltranspeptidase (γγ-GTP) were measured in blood samples by using an autoanalyser (Antech Diagnostics, Los Angeles), as described previously.[41]

2.11. *Renal function*

Blood urea nitrogen (BUN) and serum creatinine were measured in serum obtained at the time of animal sacrifice, by the Alfa Wasserman Vet-ACE autoanalyser (Alfa Wasserman Diagnostics, West Caldwell, NJ).

2.12. *Statistical analysis*

Statistical evaluation of data was done with two-tailed Student's t test. p values > 0.05 were considered not statistically significant.

3. Results and discussion

Different research groups, including ourselves, have demonstrated that unaffected lung and pleural mesothelial cells, as well as cancer cells, express nAChR.[1–13] In such experiments, α-BGT was used extensively for nAChR detection.[12] In the present series of experiments, we started assessing the number of α-BGT binding sites in IST-MES2 and MPP89 cells, determining saturation binding [Schatchard analysis (Fig. 1A panel A)]. IST-MES2 cells, as well as MPP89 cells,[12] expressed the α7-nAChR subunit (mRNAs and proteins), as observed by Western-blotting and RT-PCR experiments (Fig. 1A panels B and C). Since we already demonstrated that D-tubocurarine influences mesothelioma cell proliferation,[12] we looked at the effect of α-CbT on IST-MES2 and MPP89 cell proliferation using the colony formation assay. We first performed tests to determine binding of α-CbT to cellular nAChR. Staining for the α-CbT-FITC resulted in an important signal in the FACS analysis on the mesothelioma IST-MES2

A

Cell	n. α-BGT receptor/cells	n. experiments
A431 (positive control)	84,300.00±48.0	2 in triplicate
A549 (positive control)	17,288.6±945.8	2 in triplicate
IST-MES2	14,322.6±845.6	3 in triplicate
MPP89	17,879.13±96.47	3 in triplicate

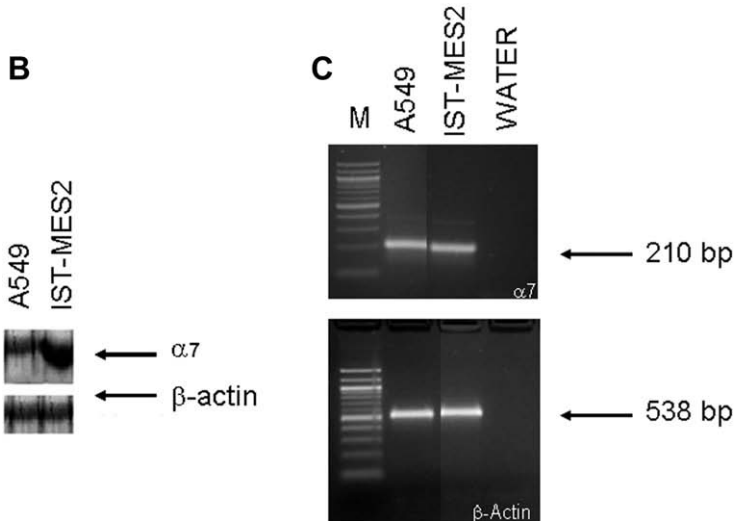

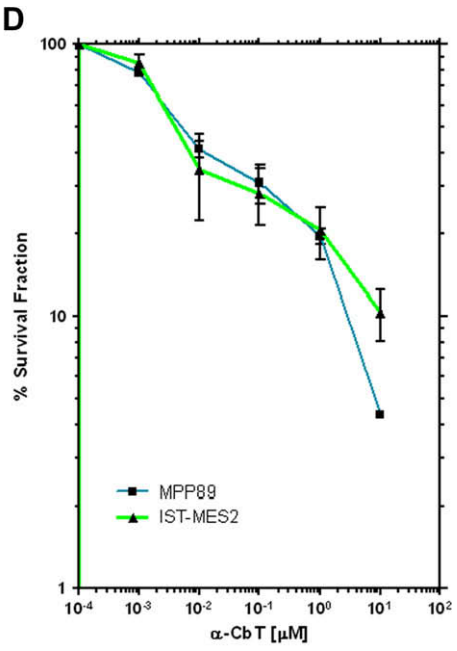

Fig. 1 – (A) Evaluation of sensitivity to α-CbT in mesothelioma cell lines IST-MES2 and MPP89. Panel A: α-BGT binding on nAChR in IST-MES2 and MPP89 cells. Mesothelioma cells were subjected to saturation binding experiments with variable amounts of [^{125}I]- α-BGT in the absence or presence of a 1000-fold excess of unlabelled α-BGT. A431 (epidermoid carcinoma) and A549 (NSCLC) cells represent positive control.[12] (B)Schatchard analysis of these binding experiments allows calculation of the number of toxin binding sites in each cell line. The figure is representative of a single experiment, which was repeated at least twice. Panel B: Western blotting and Panel C: RT-PCR for α7-nAChR carried out in IST-MES2cells. A549 (NSCLC) cells represent positive control. The figure is representative of a single experiment, which was repeated at least three times. Panel D: Clonogenic assay. IST-MES2 or MPP89 cells were plated in semisolid agar (lower 3% and upper 0.3%) and exposed to different concentrations of the drug over 18 days. 10.0 μM of medium containing α-CbT was added every 2 days. Each value [median ± SE] is representative of a single experiment, which was repeated at least three times. (B) Binding experiments with α-CbT-FITC conjugated. Experiments were performed as described previously.(C) DAPI/α-CbT-FITC double staining on MPP89 and MPP89-si-RNA-(α7-nAChR) and% survival fraction evaluation after α-CbT treatment at different concentrations.[17]

cell line (Fig. 1B). The signal significantly decreased in the presence of antibodies against α7-nAChR (epitope mapping at C-terminus). Binding was lower for human normal proliferating T lymphocytes (Fig. 1B) and super-imposable to control in resting T lymphocytes. Data in Fig. 1A, panel D, show that α-CbT (0.01-10 μM) over 18 days had some effect on cell viability. α-CbT significantly lowered the viability of IST-MES2 and MPP89 cells in a dose-dependent manner with IC_{50} values of 0.048±0.003 and 0.052±0.011 μM, respectively. Moreover, to verify the α-CbT specificity towards α7-nAChR, MPP89 cells were silenced for the receptor. Their treatment with the toxin showed a high% of survival with respect to the wild type MPP89 cells and in a DAPI/α-CbT-FITC double staining they showed a loss with a green signal specific for the α7 binding (Fig. 1C). In four different human malignant epithelioid mesotheliomas from fresh biopsy specimens (Calretinin/WT1 positive), the presence of α7-nAChR protein and mRNA were detected (Fig. 2A, B). When primary cells (RC1, RC2, GMC1, GMC2), obtained by enzymatic digestion of human mesothelioma samples, were grown in the presence of α-CbT, a marked cell-growth inhibition at the concentration of 3.0 nM was observed (Fig. 2C, D). To analyse the selectivity of α-CbT-mediated inhibition, we evaluated its effects in unaffected mesothelial cells (Mes1, Mes2) expressing α7-nAChR (Fig. 3 panels A, B). For this purpose, human normal proliferating T lymphocytes (Lym1, Lym2, Lym3), obtained from three healthy different subjects and presenting α7-nAChR, were also tested (Fig. 3 panels A and B). The results showed that treatment with α-CbT, at 0.1–10 μM for 18 days, failed to affect cell proliferation (Fig. 3 panel C). Accordingly, when human normal proliferating T lymphocytes and unaffected mesothelial cells were incubated with α-CbT at 10.0 μM for 30 h, no induction of DNA fragmentation in gel ladder experiments was observed (Fig. 3 panels D and E). Previous experiments, assessing the number of α-BGT binding sites,[12] showed that in these unaffected mesothelial cells (Mes1, Mes2), the number of α-BGT-receptors/cell was around 5000 whereas for IST-MES2 and MPP89 it was around 16,000, suggesting that cancer cells should be able to bind more molecules of α-CbT. In agreement with this observation a reduced binding of α-CbT-FITC was found in human normal proliferating T lymphocytes than in mesothelioma cells (Fig. 1B). As a consequence, the cytotoxic effects were also poorer or absent, at the same μmolar concentrations, in normal cells than in

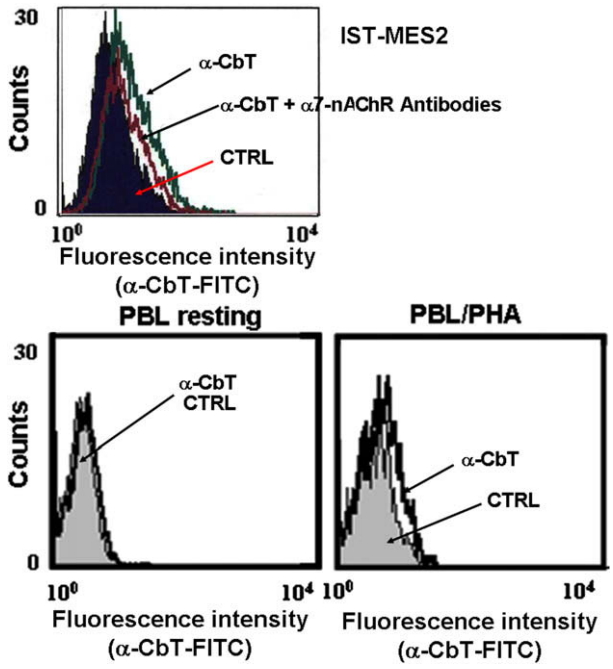

Fig. 1B.

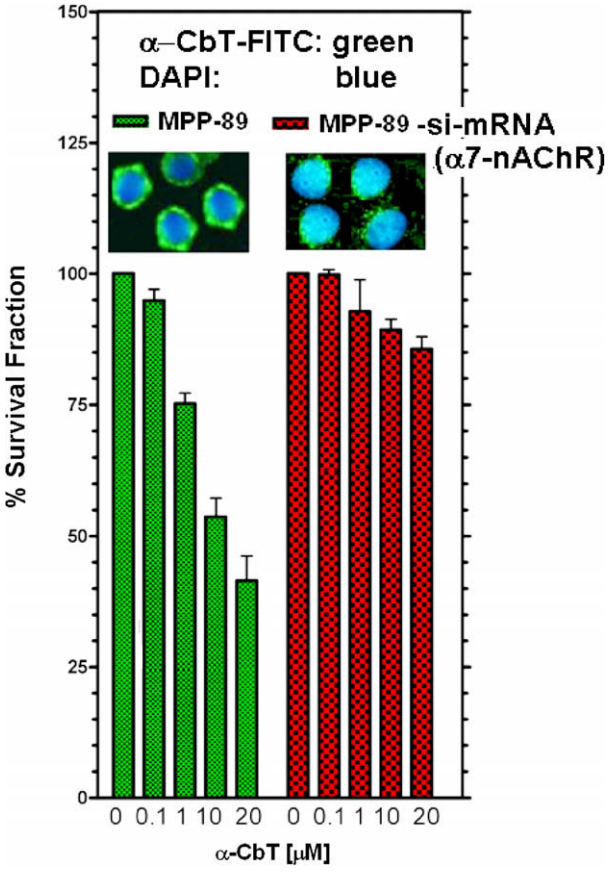

Fig. 1C.

mesothelioma cells. A previous study reported a significant relationship between higher levels of expression of the α7-nAChR, measured by [^{125}I] α-BGT binding, and increased response to 'stimuli'. In particular, while at low levels of [^{125}I] α-BGT binding, no response was observed, while intermediate levels of [^{125}I] α-BGT binding corresponded to intermediate levels of receptor function.[22] Furthermore, the study stated that there is no similar relationship between levels of expression of other nAChR and neuronal function. Interestingly, it was reported that with the condition of chronic hypoxia,[23] the cholinergic activity is largely increased. Indeed, the exposure to methyllycaconitine (50 nM), which binds to the α77-subunit of the nicotinic receptor,[24] inhibits about 50% of the hypoxia-evoked activity, and likely increases the α77-subunit of the nicotinic receptor. It is well known that regions of severe oxygen deprivation (hypoxia) arise in tumours due to rapid cell division and aberrant blood vessel formation.[25] As a result it is possible that cancer cells, under hypoxic condition, might express more cholinergic receptor than normal cells. Looking at mesotheliomas, at least two recent works,[26,27] reported the presence of hypoxia-inducible factor 1alpha (HIF-1alpha).

These results demonstrate that α-CbT selectively inhibits the growth of neoplastic mesothelial cells, sparing normal mesothelial cells.

In order to check the specificity of this inhibition, we measured the effect on cell viability of (i) a mutated α-CbT (CbT-R33E), that has been previously identified for its specific inability to interact with α7-receptor as compared to wild-type α-CbT,[28] and (ii) an analogous short-chain toxin (Erabutoxin a) specific for the muscular nAChR subtype. Despite overall structural homogeneity, curare-mimetic toxins can be divided into at least two major subfamilies on the basis of their amino acid sequences and functional properties.[1,25] One subfamily involves the long chain α-NTs with 66–74 residues and five disulfide bonds, such as α-CbT, which bind with high affinities to both α7 muscular-type and α7 neuronal nAChR. [1,29,30] The other subfamily involves short chain toxins with 60–62 residues and four disulfide bonds, which bind with high affinity to muscular-type nAChR only. In both cases, under the same experimental conditions employed in α-CbT clonogenic assay experiments described in Fig 1A, panel D, drugs did not affect cell growth (% survival fraction > 94–97%, respectively), confirming the specificity of the α-CbT effect on the α7-neuronal receptor.

This experiment suggests that the cytotoxic activity in mesothelioma cells is correlated to the inhibition of neuronal-type α7-nAChR rather than muscular-type nAChR. Additionally, we recently reported that α-CbT did not affect mongoose cell (AP cell) growth.[21] As already reported,[31] sequences of the α-subunits of the nAChR from mongoose contain several differences in the region between amino acids 183 and 200, which confer resistance on this species to the snake α-toxins. In binding experiments, neither binding of α-CbT FITC-conjugated nor growth decrease were observed after 72 h of continuous exposure.[21] Finally, when experiments were performed on the presence of α7-nAChR antibodies, the survival fraction of CbT-treated cells was greater than 90%.

We then assessed whether the cell growth inhibitory effect induced by α-CbT on mesothelioma cells was associated with induction of apoptosis. Experiments were performed in

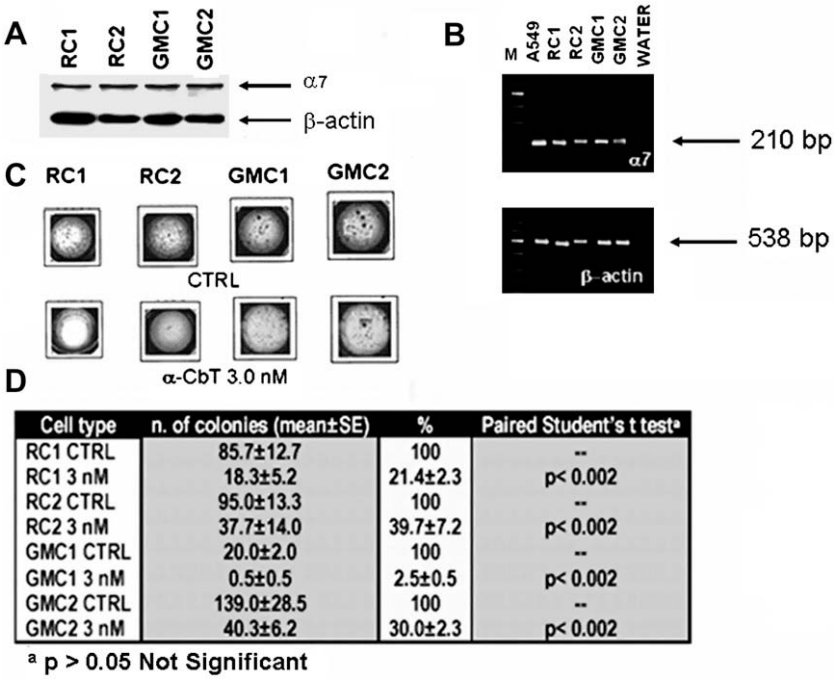

Cell type	n. of colonies (mean±SE)	%	Paired Student's t test[a]
RC1 CTRL	85.7±12.7	100	--
RC1 3 nM	18.3±5.2	21.4±2.3	p< 0.002
RC2 CTRL	95.0±13.3	100	--
RC2 3 nM	37.7±14.0	39.7±7.2	p< 0.002
GMC1 CTRL	20.0±2.0	100	--
GMC1 3 nM	0.5±0.5	2.5±0.5	p< 0.002
GMC2 CTRL	139.0±28.5	100	--
GMC2 3 nM	40.3±6.2	30.0±2.3	p< 0.002

[a] p > 0.05 Not Significant

Fig. 2 – Evaluation of sensitivity to α-CbT in human mesothelioma cells in primary culture (RC1, RC2, GMC1, and GMC2). Panel A: Western blotting and Panel B: RT-PCR for α7-nAChR carried out in mesothelioma RC1, RC2, GMC1, GMC2 cells. The figure is representative of a single experiment, which was repeated at least three times. Panel C: Photographs of colonies grown on semisolid agar from α-CbT -treated or untreated cells. Cells were exposed to 3.0 nM α-CbT over 18 days. 10.0 μM of medium containing α-CbT was added every 2 days. The figure is representative of a single experiment, which was repeated at least three times. Panel D: n. of colonies (mean ± SE of three independent experiments performed in triplicate) and% survival fraction of mesothelioma cells in primary culture (RC1, RC2, GMC1, and GMC2) exposed to α-CbT.

IST-MES 2 cells. The loss of mitochondrial membrane potential (ΔΔΨΨ) is one hallmark of apoptosis. It is an early event preceding phosphatidylserine externalisation and coinciding with caspase activation. JC-1 dye is used to measure ΔΔΨΨ in cells. In non-apoptotic cells, JC-1 accumulates as aggregates in the mitochondria, resulting in red fluorescence. The brightness of red fluorescence is proportional to ΔΔΨΨ and varies among different types. However, in apoptotic and necrotic cells, JC-1 exists in monomeric form and stains cells green. As shown in Fig. 4 panel A, α-CbT treatment resulted in a dose- and time-dependent change of ΔΔΨΨ. The maximum effects were obtained with 1.0 μM α-CbT administered for 30 h. This concentration induced cleavage of caspase-3, measured both fluorometrically (Fig. 4 panel B) and by Western blotting (Fig. 4 panel C). α-CbT-apoptosis-induction was confirmed by microscopic observation of the cells labelled with DAPI (Fig. 5 panel A). α-CbT treatment resulted in a dose-dependent apoptosis in IST-MES2 cells, with an increasing trend of apoptotic cells at 0.3 μM treatment (Fig. 5 panel A). The induction of apoptosis was negligible at the lowest α-CbT dose (0.1 μM), and impressive at the highest dose employed (10 μM). A similar trend was revealed when apoptosis was measured by ladder formation on agarose gel electrophoresis (Fig. 5 panel B); in the presence of caspase-3 inhibitor, no effect was observed (far right lane in the gel of Fig 5 panel B). We next quantified the extent of apoptosis by flow cytometric analysis using Annexin V-PI. IST-MES2 cells, treated with α-CbT 1.0 μM for 30 h, resulted in 28.4±4.2% necrotic or late apoptotic; whereas 54.2±5.7% were early apoptotic as compared to 8.2±1.4% and 2.9 ±0.3% of untreated cells (Fig. 5 panel C). It is important to note that normal cells (human T lymphocytes and unaffected mesothelial cells) did not appear apoptotic when treated with α-CbT 10.0 μM for 30 h (Fig. 3 panels D and E) suggesting the susceptibility of mesothelioma cells to undergo apoptosis in the presence of α-CbT.

The effect of the α-CbT on the levels of IAP (Inhibitors of Apoptosis Protein) was estimated by RT-PCR and Western blotting. Survivin, one IAP family gene member, is highly over expressed in mesothelioma.[32] Survivin crosses multiple signalling networks implicated in inhibition of apoptosis principally by targeting the intrinsic (i.e. mitochondrial) pathway of cell death interfering with caspase-9 processing, the upstream initiation of the intrinsic pathway.[33] Recently, survivin up-regulation was assumed to be an essential mediator of nicotine-inhibition of apoptosis induced by chemotherapeutic drugs in A549 cells.[34] In the next series of experiments, we analysed the effect of α-CbT on mRNA and protein expression of some IAP family gene members (survivin, XIAP, IAP2, and IAP1). In a dose-dependent study, we found that treatment of IST-MES2 cells with α-CbT resulted in a marked decrease of IAPs mRNA and protein expression (Fig. 6). The dose-dependent effect of α-CbT on IST-MES2 cells showed a significant decrease in IAPs mRNA (Fig. 6 panels A and B) and protein expression (Fig. 6 panels C and D) at 1.0 μM 30 h post-treatment. Densitometric analysis of the data of Fig. 6, panels C and D, revealed that the decrease was 75% for survi-

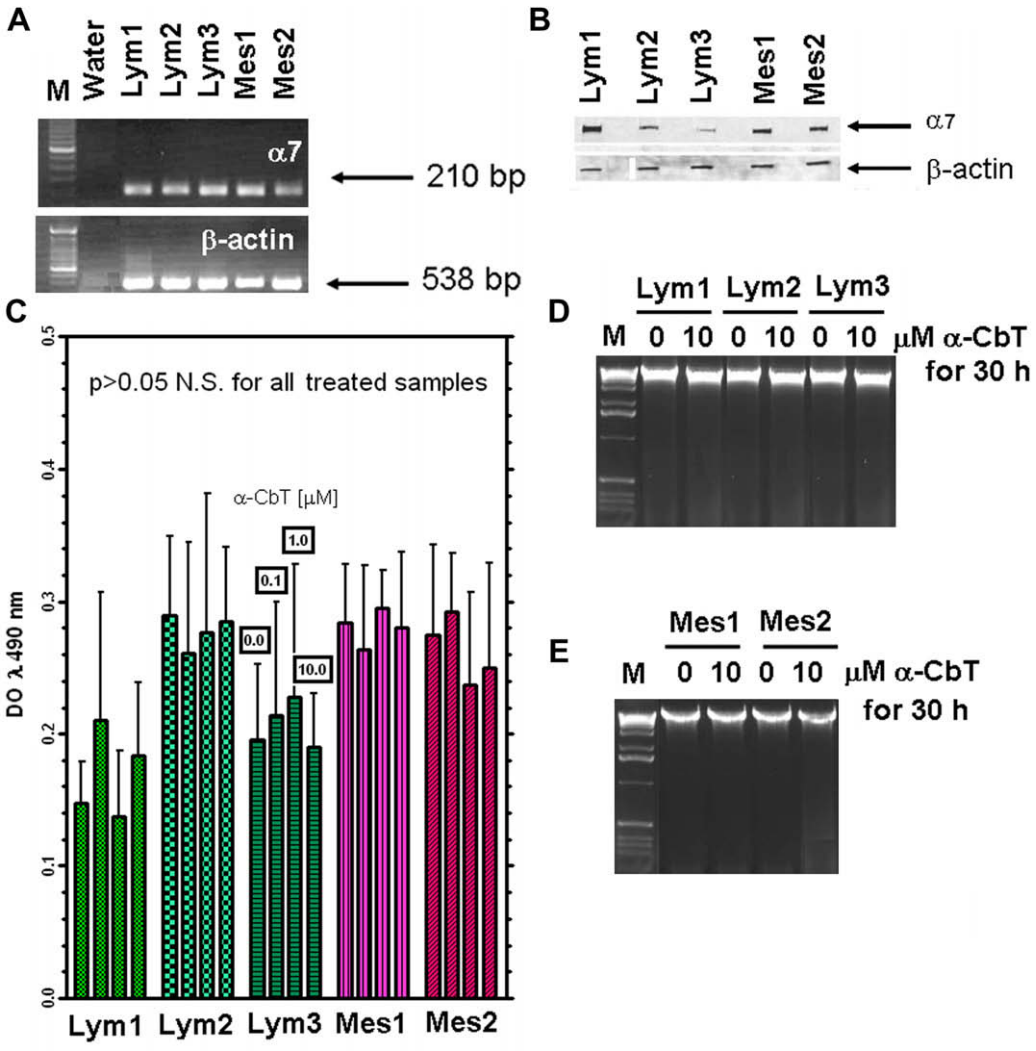

Fig. 3 – Evaluation of sensitivity to α-CbT on unaffected human mesothelial cells obtained by two different subjects (Mes1, Mes2) and on proliferating (PHA/IL2 stimulated) human T lymphocytes obtained from three healthy donors (Lym1, Lym2, and Lym3). Panel A: RT-PCR and Panel B: Western blotting for α7-nAChR. The figure is representative of a single experiment, which was repeated at least three times. Panel C: MTS assay on proliferating (PHA/IL2 stimulated) human T lymphocytes and human mesothelial cells. The MTS assay was performed as described previously.[34] Data are plotted as mean ± SE of three independent experiments performed in triplicate. Statistical evaluation of data was done with two-tailed Student's t-test. Panel D: Internucleosomal DNA fragmentation. (PHA/IL2 stimulated) Human T lymphocytes (Lym1, Lym2, and Lym3) were incubated with α-CbT for 30 h. Panel E: Internucleosomal DNA fragmentation. Human mesothelial cells (Mes1, Mes2) were incubated with α-CbT for 30 h. M: marker. The figures are representative of a single experiment, which was repeated at least three times.

vin, 90% for XIAP, 98% for IAP1 and IAP2 proteins. All these observations support the hypothesis that IST-MES2 cell proliferation requires α7-nAChR function. However, Dasgupta et al.[34] reported that α-BGT (α7 antagonist) was unable to prevent nicotine-mediated inhibition of apoptosis (in contrast to inhibitors of α33ββ22 and α44ββ22 subunits) suggesting that these last subunits are involved in the process. This difference might be linked to the observations that nicotine by itself did not change the regulation of survivin and XIAP.[34]

We also examined the effect of α-CbT on BCL-XL expression. Different authors, including ourselves, reported that BCL-XL is over expressed in mesothelioma.[35,36] The BCL-2 family proteins, controlling critical events at the beginning of apoptosis, consist of three subfamilies: the proapoptotic (Bax), the antiapoptotic (BCL-2) and the BH-3 subfamily. The BCL-2 subfamily includes BCL-XL. The switching on and off of apoptosis is determined by the ratio between proapoptotic and antiapoptotic proteins.[34] In the NCI-ACDS study,[35] a strong negative correlation was reported between basal BCL-XL protein and mRNA levels and drug sensitivity, suggesting that BCL-XL may play a unique role in general resistance to cytotoxic agents. In view of these data, it is not surprising that mesothelioma is considered strongly resistant to drugs. α-CbT caused a significant decrease of BCL-XL mRNA (Fig. 6 panel B) and protein expression (Fig. 6 panel D) in IST-MES2 cells as revealed by densitometric analysis, since 1.0 μM α-CbT for 30 h decreased proteins by ~85%.

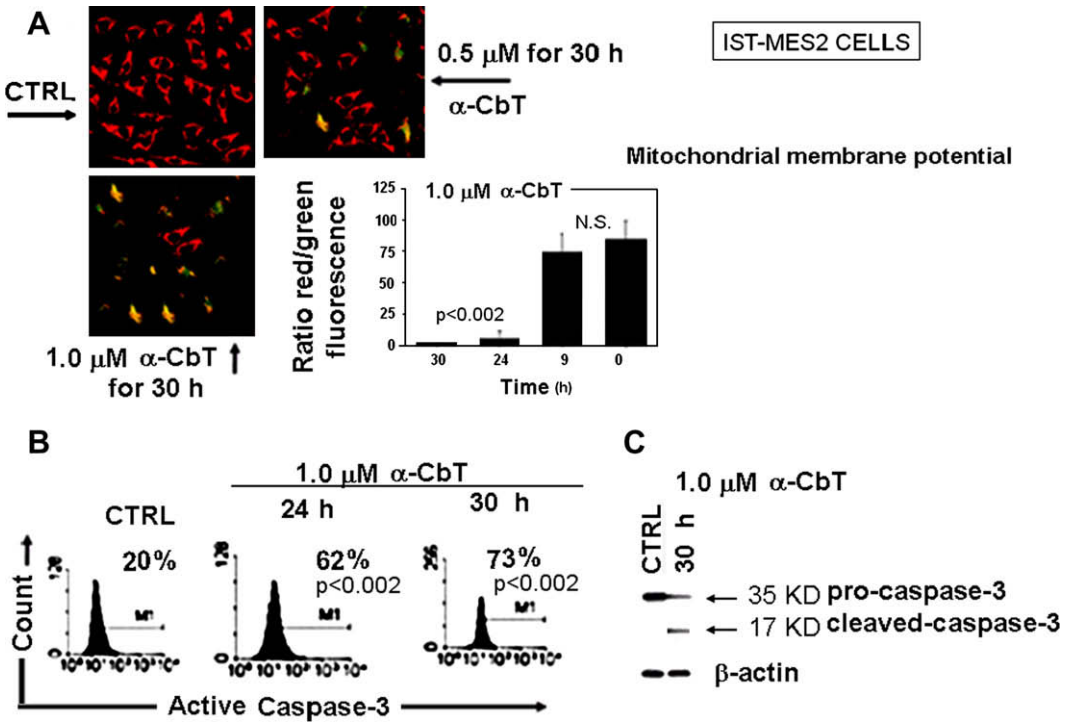

Fig. 4 – Apoptosis induction and regulation in IST-MES2 cells. Panel A: Mitochondrial membrane potential was measured using the JC-1 kit according to the manufacturer's instructions. Statistical evaluation of data was done with two-tailed Student's t-test. The figure is representative of a single experiment, which was repeated at least three times. Panel B: Cells were treated with 1.0 μM of α-CbT for 24 or 30 h for caspase-3 activation. Enzymatic activity of caspase-3-like proteases was determined by incubation of 10 μg of total protein with its specific fluorogenic substrate (Ac-DEVD-MCA), for 2 h at 37 °C; cells were then analysed by flow cytometry (FACSCalibur), and the increase of caspase activity was determined after proper gating in comparison with untreated cells.[41] The figure is representative of a single experiment, which was repeated at least three times. Panel C: Caspase-3 activation determined by Western blotting, as described previously(41) The figure is representative of a single experiment, which was repeated at least three times.

To assess *in vivo* the antitumour effects of α-CbTIST-MES2 and MPP89 mesothelioma cell lines, and GMC1 and RC1 mesothelioma primary cells, were grown as xenografts in NOD/SCID mice orthototopically xenotransplanted. All mice developed macroscopic tumours within 20–30 days.

The acute (5 days) i.v. LD_{50} of α-CbT was 0.15 mg/kg (LD_{10} = 0.12; LD_{90} = 0.20 mg/kg). These doses were selected following treatment of 50 NOD/SCID mice with different concentrations of α-CbT (from 0.004 to 0.24 mg/kg). 0.004 and 0.04 mg/kg were the lowest experimental doses causing no lethality. Mice treated with 0.24 mg/kg (LD_{100}) died from fatal respiratory failure and massive kidney necrosis (Fig. 7 panel A). Indeed, adrenal gland (Fig. 7 panel A, pictures a and b) showed necrosis and haemorrhages involving both cortex and medulla with presence of some apoptotic cells. In the kidney (Fig. 7 panel A, pictures c and d) tubular necrosis associated with haemorrhage was the main histomorphological finding. Liver (Fig. 7 panel A, picture e) showed only diffuse dilatation of the central veins, whilst lung (Fig. 7 panel A, picture f) had focal alveolar haemorrhage and perivascular and interstitial transudate, with oedematous widening of alveolar septa. The LD_{50} that we found in NOD/SCID mice (0.15 mg/kg) is in the range of values described in the literature for α-CbT (0.1–0.3 mg/kg) and is close to that reported by Pergolizzi et al.[36] It has to be noted that in Pergolizzi's experiments, 2.0 μg i.v. induces 80% lethality in BalB-C mice (20 g). It is important to known that inbred mouse strains differ in their levels of brain α-BGT binding sites and these differences correlate with different animal sensitivity to nicotine.[40] Restriction fragment length polymorphisms at the α7 locus and strain-specific polymorphisms were identified, suggesting that α7 genotype is an important determinant of α-BGT receptor levels.[40]

To assess long term toxicity, 12 non-grafted NOD/SCID mice (four animals for each experiment) were treated three times a week with α-CbT 0.12 ng/kg (1/1000 of LD_{10}) administered i.v. for 2 months. In treated mice we did not observe any lethality or toxicity such as: histological alterations (Fig. 7 panel B), body and organ weight loss (Fig. 7 panel C), serum chemistry alterations (Fig. 8 panel A), haematological alterations (Fig. 8 panel B), serum kidney (Fig. 8 panel B) and liver enzymes (Fig. 8 panel C). Fig. 7 panel B shows histological normal tissue of liver (a), pancreas (b), lung (c), kidney (d) and CNS (e and f) after long term treatment. Moreover, mice were examined for neurological effects assessing autonomic, convulsive, excitability, neuromuscular, sensory-motor and general motor activity domains. Treatment-related effects were not observed in these domains for any of the treated groups of mice compared to the controls.

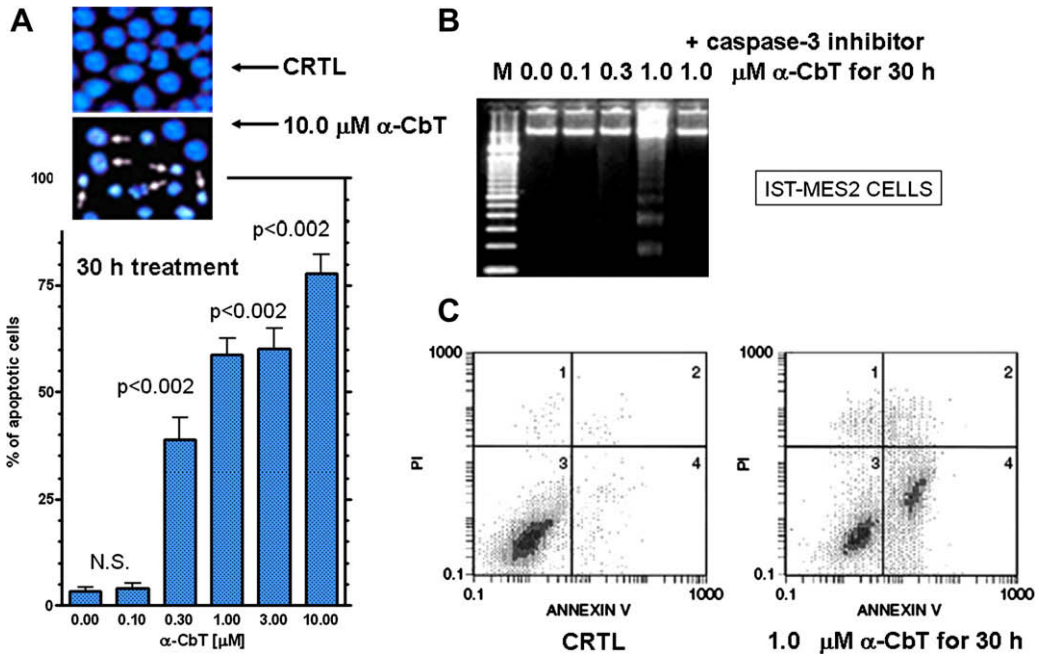

Fig. 5 – Apoptosis evaluation in IST-MES2 cells. Cells were treated with different concentrations of α-CbT for 30 h. Panel A: Apoptotic cells were evaluated by DAPI staining. Data are plotted as mean ± SE of three independent experiments performed in triplicate. Statistical evaluation of data was done with two-tailed Student's t-test. The figure on top of the graph is representative of a single experiment, which was repeated at three times. Panel B: Internucleosomal DNA fragmentation. Cells loaded on the far right lane in the gel were pre-incubated with caspase-3 inhibitor. The figure is representative of a single experiment, which was repeated at least three times. Panel C: Apoptosis was identified by staining with Annexin V (x-axis) and PI (y-axis). Cells binding Annexin V and retaining PI were apoptotic (quadrant n.4); double-positive cells underwent secondary necrosis (quadrant n. 2). Data are representative of three replicate experiments yielding similar results.

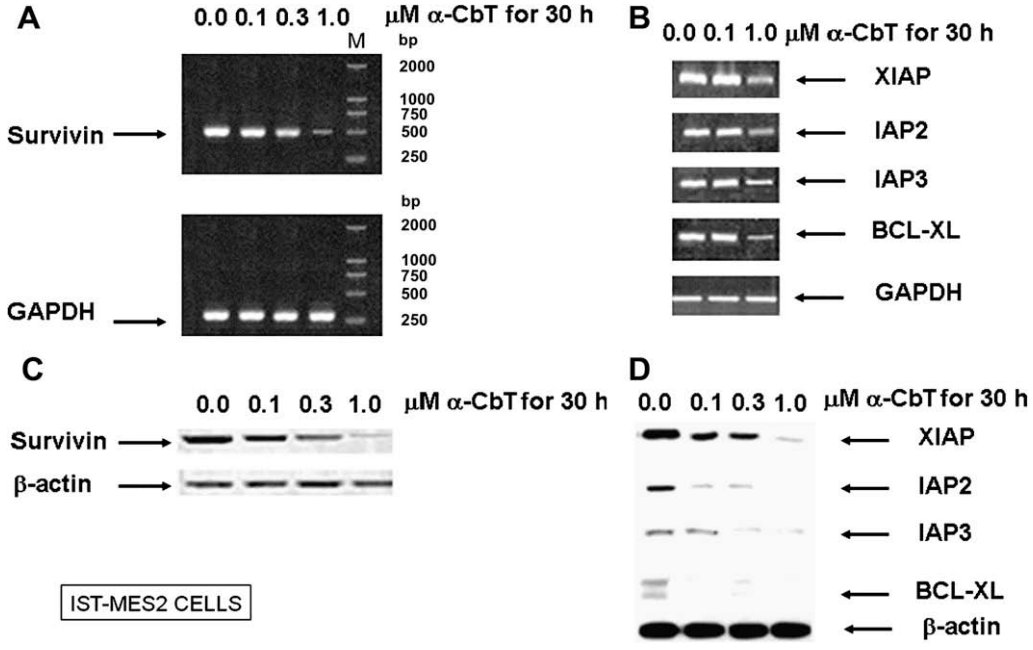

Fig. 6 – Regulation of the expression of IAPs in IST-MES2 cells. Cells were treated with different concentrations of α-CbT for 30 h. Panel A and Panel B: RT-PCR and Panel C and Panel D: Western blotting for survivin, XIAP, IAP2, IAP1 and BCL-XL. Data are representative of three replicate experiments yielding similar results. M: marker.

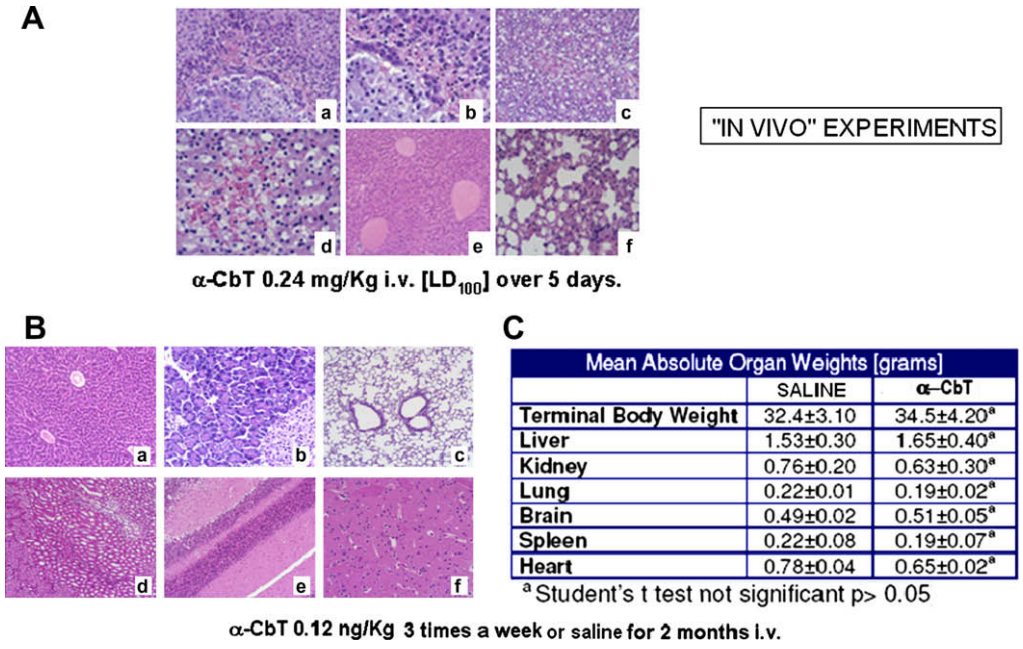

Fig. 7 – Evaluation of α-CbT toxicity in NOD/SCID mice. Panel A: Haematoxylin and eosin (H&E) of tissues from mice treated i.v. with the LD_{100} of α-CbT observed with an Olympus B40 microscope (magnification 100×). Adrenal gland (a and b), kidney (c and d), liver (e) and lung (f). Panel B: H&E of tissues from mice treated with α-CbT 0.12 ng/ml (1/1000 of LD_{100}) observed with an Olympus B40 microscope (magnification 100×). Liver (a), pancreas (b), lung (c), kidney (d), and central nervous system (e and f). Panel C: Organ weights of mice treated as in panel B.

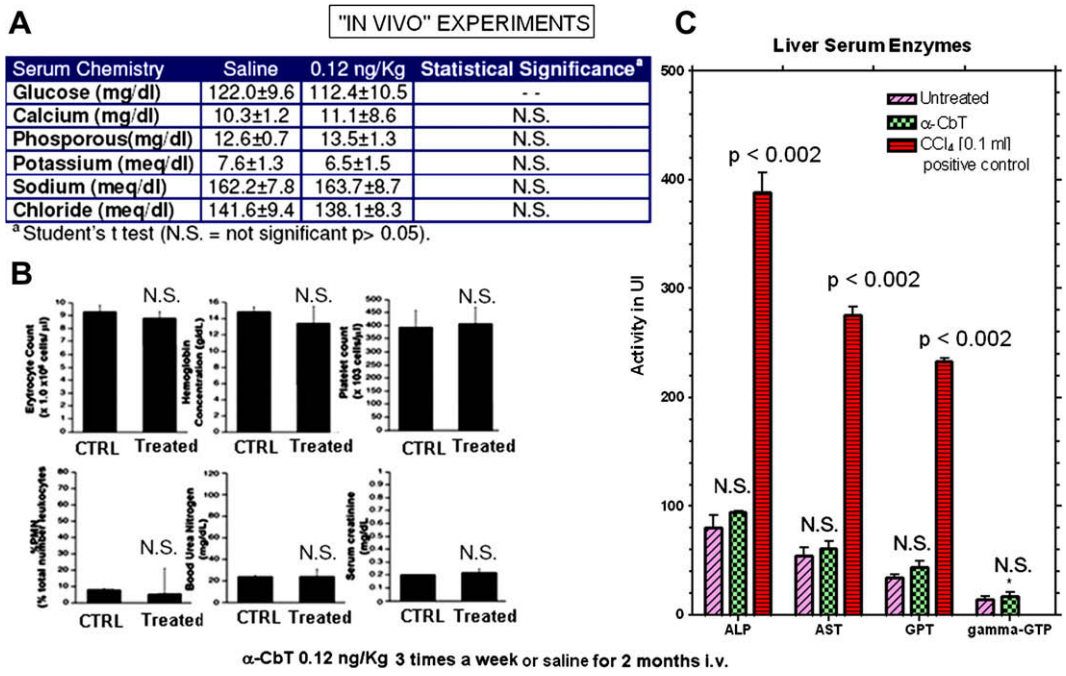

Fig. 8 – Evaluation of α-CbT toxicity in NOD/SCID mice. Mice were treated as in Fig. 7, panel B. Panel A: Serum clinical chemistry; Panel B: Erythrocyte and platelet counts,% PMN, haemoglobin, BUN and serum creatinine concentrations; Panel C: Serum levels of aspartate aminotransferase (AST), alkaline phosphatase (ALP), glutamic pyruvic transaminase (GPT) and α-glutamyltranspeptidase (α-GTP). Data are plotted as mean ± SE. Statistical evaluation of data was done with two-tailed Student's t-test.

In a further experiment, nine out of 18 mice were grafted with IST-MES2 cells, six out of 12 with MPP89 cells, six out of 12 with GMC1 cells and five out of 11 with RC1 cells. Animals were treated three times a week, with α-CbT 0.12 ng/kg

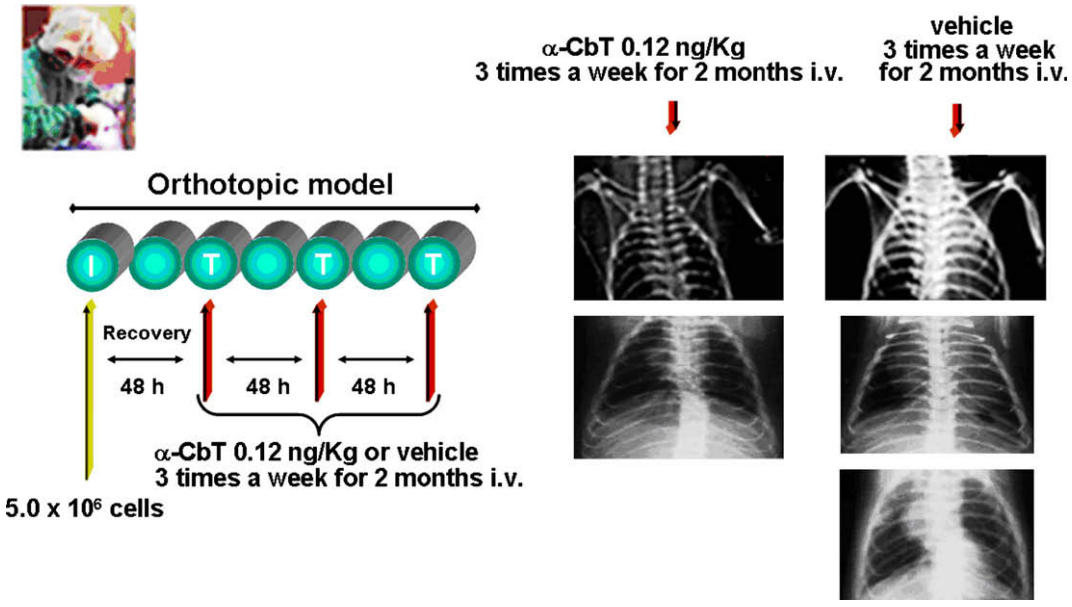

Fig. 9 – (A) *In vivo* antitumour activity of α-CbT in mesothelioma transplanted NOD/SCID mice. On the left: Planning of experiments. Female NOD/SCID mice (NOD/SCID/NOD/SCID 8-week-old, born and maintained in our Animal Facility Center) were grafted orthotopically with different mesothelioma cells (IST-MES2 or MPP89or GMC1or and RC1). 48 h after grafting, mice were randomised in two groups. The control group received vehicle alone and the treated group α-CbT 0.12 ng/ml [1/1000 of LD_{100}] three times a week i.v. for 2 months. After 2 months, anaesthetised mice were subjected to chest x-ray examinations and autopsy. On the right: Mice transplanted with IST-MES2 cells (as an example). Chest x-rays show large radiopaque left mediastinal mass and gross examinations of vehicle alone treated group show various nodules at different locations on the parietal pleural (different pictures, with different magnifications). (B) Macroscopic and microscopic examination. At histopathological examination, nodules showed typical histology of epithelioid mesothelioma (H&E and Calretinin positive immunohistochemistry. (C) Number of α-CbT and vehicle alone treated mice developing tumours. (D, E) Determination of mice body weights during the treatment period. Data are plotted as mean ± SE. Statistical evaluation of data was done with two-tailed Student's t-test. (F) *In vivo* antitumour activity: α-CbT treatment of mesothelioma transplanted NOD/SCID mice started in a late phase of tumour progression.

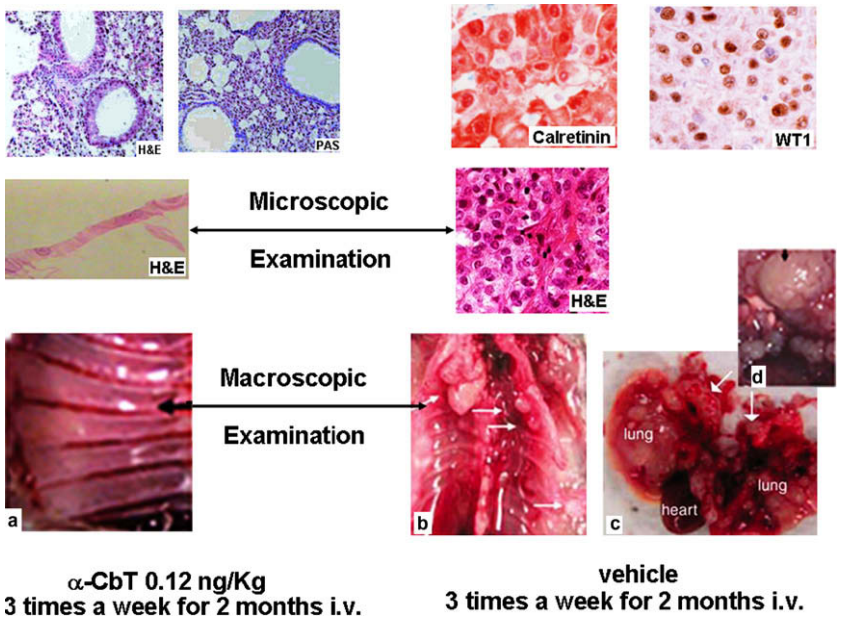

Fig. 9B.

(1/1000 of LD_{10}) administered i.v. for 2 months. Vehicle-treated animals served as controls in each group. Treatment started 2 days after cell implantation (Fig. 9A, on the left). Mice chest X-rays, taken before autopsies, were blindly read and described based on the extent of the observed abnormalities (mediastinum widening, loss of cardiac silhouette with subcardiac clear space filling and mass deformity of the diaphragm area). After 2 months, macroscopic, microscopic and chest x-ray features of massive tumour volumes were observed in all control mice (Fig. 9A, on the right) whereas no abnormalities were observed in α-CbT treated mice (Fig. 9A, on the right). At autopsy, all control mice (vehicle-treated) exhibited massive tumours predominantly invading the mediastinum and pericardium and involving the diaphragm (Fig. 9B, on the right). An extension to the lungs was occasionally found. Tumour metastases were not found in the visceral organs. Fig. 9C shows that α-CbT had inhibited the development and the growth of tumours in all treated mice (no presence of tumours evaluated after gross examinations and H&E analyses of pleural, lung mediastinum, pericardium and diaphragm). H&E analyses did not reveal scattered areas of mesothelioma formation (Fig. 9B). Moreover, control mice developed tumour cachexia, as documented by progressive body weight loss, while treated mice grew regularly (Fig. 9D, E).

Furthermore, 20 mice (five per group/two experiments) were transplanted with MPP89-Luc cells in order to mimic, at best, the real clinical setting of malignant pleural mesothelioma that is mostly diagnosed in its progressive stage. The animals' drug treatment was initiated when the tumours were well established at day 14 and the final end-point had been set to be the survival of each of the mesothelioma–bearing NOD/SCID mice instead of the reduction of tumour masses as previously evaluated (Fig. 9F). The α-CbT treatment enhanced the animal survival rate by almost four times (120 days versus 32 days).

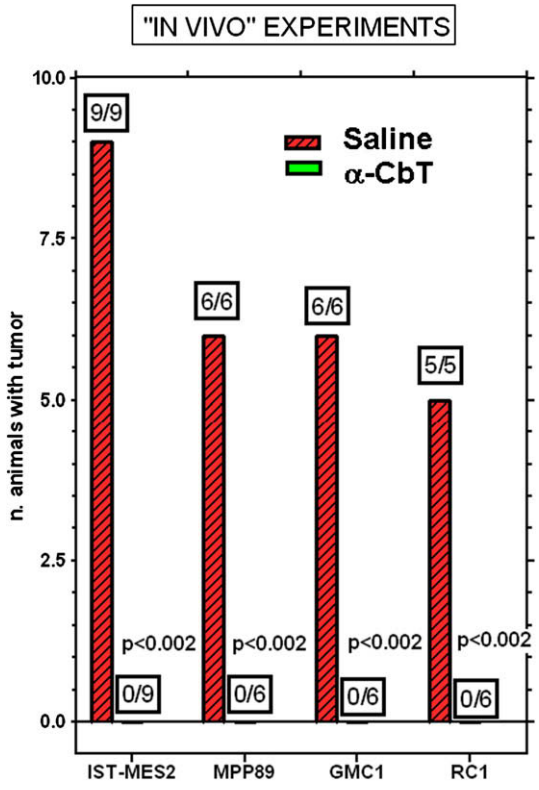

Fig. 9C.

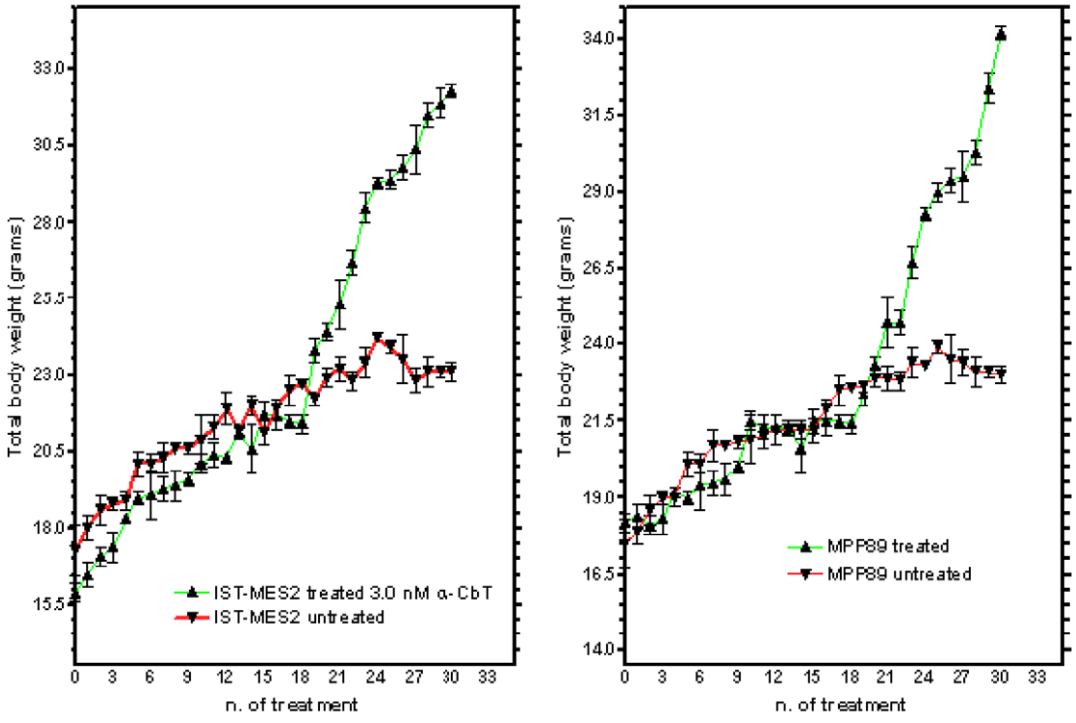

Fig. 9D.

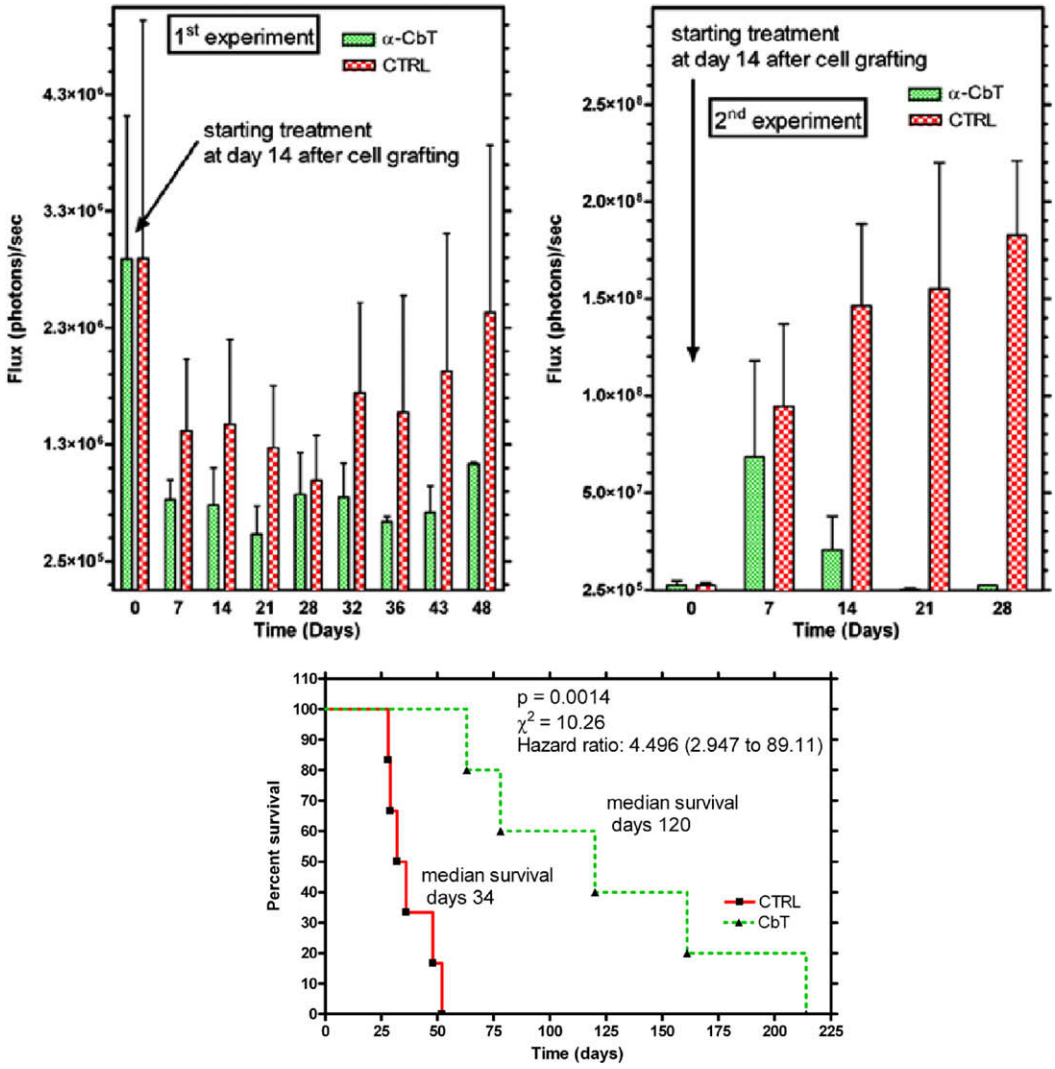
1st experiment
α-CbT
CTRL
starting treatment
at day 14 after cell grafting
Flux (photons)/sec
Time (Days)
2nd experiment
p = 0.0014
χ2 = 10.26
Hazard ratio: 4.496 (2.947 to 89.11)
median survival
days 120
median survival
days 34
CTRL
CbT
Percent survival
Time (days)

Fig. 9E.

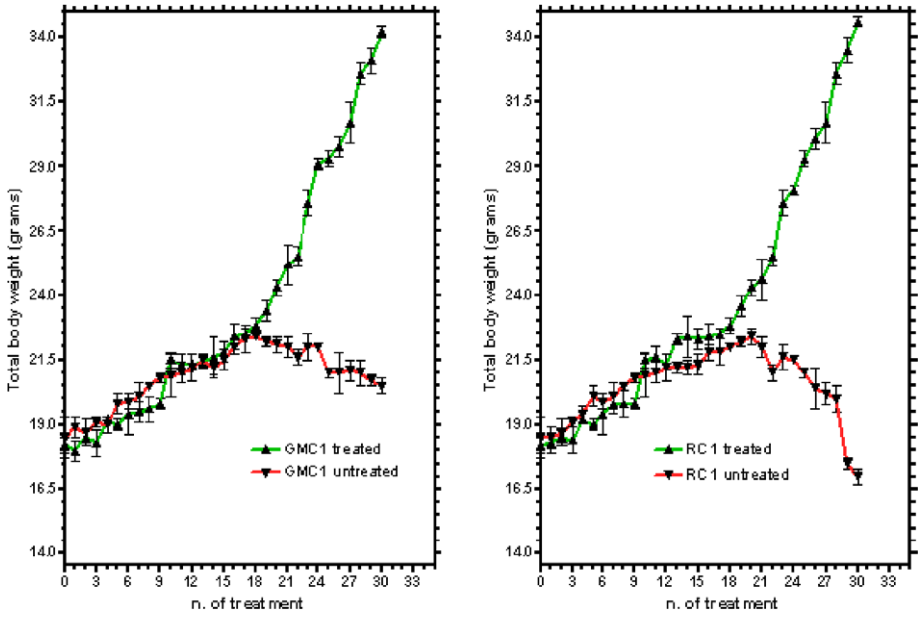
Total body weight (grams)
GMC1 treated
GMC1 untreated
RC1 treated
RC1 untreated
n. of treatment

Fig. 9F.

Based on the results reported above we can conclude that α-CbT, a high affinity antagonist of α7-nAChR, induces a significant inhibitory effect on the growth of mesothelioma. Additional studies are needed to further understand the complex α7-nAChR-antagonist system in cancer cells and to evaluate α7-nAChR as a potential target in cancer therapy. In our *in vivo* tumour model, α-CbT treatment began 48 h after grafting mesothelioma cells, in the absence of vasculature support and when the cells were loosely implanted or possibly not implanted at all. The possibility exists that resistant cells might be selected after implantation; therefore, further experiments need to be warranted to evaluate the antitumour effects of α-CbT in an *in vivo* model of mesothelioma whose pleural implantation is firmly established.

The idea to use venom peptides as therapeutical agents in the treatment of human diseases is not new; snake venom derived compounds (peptides-proteins) have been used as lead molecules to develop novel strategies in antithrombotics, antihaemorrhagic, antihypertensive or defibrinogenating therapy.[1,41] To the best of our knowledge these compounds have not been fully investigated for possible anticancer therapy in animal models, nor has their mechanism of action, as antitumour drugs, been elucidated. Our results suggest the exploitation of the α-CbT molecule as a leading compound for the development of possible antitumour agents for mesothelioma. Non-immunogenic derivatives of the α-CbT molecule need to be developed in order to optimise a possible drug design.

Conflict of interest statement

None declared.

Acknowledgments

Grant support: Fondazione "Paola Giancola per la Ricerca sul Cancro" Varese Italy 2005. Dr. Alessia Catassi received a fellowship from Associazione Italiana per la Ricerca sul Cancro (Comitato Ligure) Milan Italy.

REFERENCES

1. Russo P, Catassi A, Cesario A, Servent D. Development of novel therapeutic strategies for lung cancer: targeting the cholinergic system. *Curr Med Chem* 2006;**13**:3493–512.
2. Paleari A, Grozio A, Cesario A, Russo P. The cholinergic system and cancer. Sem Cancer Biol [in press].
3. Catassi A, Paleari L, Cesario A, Russo P. Nicotine: a single agent in lung cancer induction and progression. Mut Res-Rev [in press].
4. Minna JD. Nicotine exposure and bronchial epithelial cell nicotinic acetylcholine receptor expression in the pathogenesis of lung cancer. *J Clin Invest* 2003;**111**:31–3.
5. Maus AD, Pereira EF, Karachunski PI, et al. Human and rodent bronchial epithelial cells express functional nicotinic acetylcholine receptors. *Mol Pharmacol* 1998;**54**:779–88.
6. Zia S, Ndoye A, Nguyen VT, Grando SA. Nicotine enhances expression of the alpha 3, alpha 4, alpha 5, and alpha 7 nicotinic receptors modulating calcium metabolism and regulating adhesion and motility of respiratory epithelial cells. *Res. Commun Mol Pathol Pharmacol* 1997;**97**:243–62.
7. Maneckjee R, Minna JD. Opioid and nicotine receptors affect growth regulation of human lung cancer cell lines. *Proc Natl Acad Sci U S A* 1990;**87**:3294–8.
8. Plummer HK III, Dhar M, Schuller HM. Expression of the alpha7 nicotinic acetylcholine receptor in human lung cells. *Respir Res* 2005;**6**:29–38.
9. Wang Y, Pereira EF, Maus AD, et al. Human bronchial epithelial and endothelial cells express alpha7 nicotinic acetylcholine receptors. *Mol Pharmacol* 2001;**60**:1201–9.
10. Schuller HM. Cell type specific, receptor-mediated modulation of growth kinetics in human lung cancer cell lines by nicotine and tobacco-related nitrosamines. *Biochem Pharmacol* 1989;**38**:3439–42.
11. West KA, Brognard J, Clark AS, et al. Nicotine induces cell proliferation by beta-arrestin-mediated activation of Src and Rb-Raf-1 pathways. *J Clin Invest* 2006;**6**:2208–17.
12. Trombino S, Cesario A, Margaritora S, et al. Alpha7-nicotinic acetylcholine receptors affect growth regulation of human mesothelioma cells: role of mitogen-activated protein kinase pathway. *Cancer Res* 2004;**64**:135–45. Erratum in: Cancer Res 2004; 64:1559.
13. Lam DC, Girard L, Ramirez R, et al. Expression of nicotinic acetylcholine receptor subunit genes in non-small-cell lung cancer reveals differences between smokers and nonsmokers. *Cancer Res* 2007;**67**:4638–47.
14. Calmette A, Saenz A, Costil L. Du venin de cobra sur les greffes cancéréuses et sur le cancer spontané (adénocarcinome) de la souris. *CR Acad Sci* 2003;**197**:205.
15. Seliger H. New results with cobratoxin in cancer therapy. *Med Welt* 1951;**20**:638.
16. Grozio A, Catassi A, Cavalieri Z, et al. Nicotine, lung andcancer. *Anticancer Agents Med Chem* 2007;**7**:461–6.
17. Grozio A, Paleari L, Catassi A, et al. Natural agents targeting the alpha7-nicotinic-receptor in NSCLC: A promising prospective in anti-cancer drug development. *Int J Cancer* 2007.
18. Orengo AM, Spoletini L, Procopio A, et al. Establishment of four new mesothelioma cell lines: characterization by ultrastructural and immunophenotypic analysis. *Eur Respir J* 1999;**13**:527–34.
19. Antil-Delbeke S, Gaillard C, Tamiya T, et al. Molecular determinants by which a long chain toxin from snake venom interacts with the neuronal alpha 7-nicotinic acetylcholine receptor. *J Biol Chem* 2000;**275**:29594–601.
20. Trombino S, Cesario A, Margaritora S, et al. Alpha7-nicotinic acetylcholine receptors affect growth regulation of human mesothelioma cells: role of mitogen-activated protein kinase pathway. *Cancer Res* 2004;**64**:135–45.
21. Oates J, Edwards C. HBME-1, MOC-31, WT1 and calretinin: an assessment of recently described markers for mesothelioma and adenocarcinoma. *Histopathology* 2000;**36**:341–7.
22. Stevens KE, Freedman R, Collins AC, et al. *Neuropsychopharmacol* 1996;**15**:152–62.
23. He L, Dinger B, Fidone S. Effect of chronic hypoxia on cholinergic chemotransmission in rat carotid body. *J Appl Physiol* 2005;**98**:614–9.
24. Davies AR, Hardick DJ, Blagbrough IS, et al. Characterisation of the binding of [3H]methyllycaconitine: a new radioligand for labelling alpha 7-type neuronal nicotinic acetylcholine receptors. *Neuropharmacol* 1999;**38**:679–90.
25. Keith B, Simon MC. Hypoxia-inducible factors, stem cells, and cancer. *Cell* 2007;**129**:465–72.
26. Klabatsa A, Sheaff MT, Steele JP, et al. Expression and prognostic significance of hypoxia-inducible factor 1alpha (HIF-1alpha) in malignant pleural mesothelioma (MPM). *Lung Cancer* 2006;**51**:53–9.

27. Singhal S, Wiewrodt R, Malden LD, et al. Gene expression profiling of malignant mesothelioma. *Clin Cancer Res* 2003;**9**:3080–97.
28. Karlsson E, Arnberg H, Eaker D. Isolation of the principal neurotoxins of two Naja naja subspecies. *Eur J Biochem* 1971;**15**:1–16.
29. Servent D, and Ménez A Massaro EJ (Ed.). Handbook of neurotoxicology, Humana press Inc: Totowa, NJ; pp-385-425.
30. Keller SH, Kreienkamp HJ, Kawanishi C, Taylor PL. Molecular determinants conferring alpha-toxin resistance in recombinant DNA-derived acetylcholine receptors. *J Biol Chem* 1995;**270**:4165–71.
31. Falleni M, Pellegrini C, Marchetti A, et al. Quantitative evaluation of the apoptosis regulating genes Survivin, Bcl-2 and Bax in inflammatory and malignant pleural lesions. *Lung Cancer* 2005;**48**:211–6.
32. Wheatley SP, McNeish IA. Survivin: a protein with dual roles in mitosis and apoptosis. *Int Rev Cytol* 2005;**247**:35–88.
33. Dasgupta P, Kinkade R, Joshi B, et al. Nicotine inhibits apoptosis induced by chemotherapeutic drugs by up-regulating XIAP and survivin. *Proc Natl Acad Sci U S A* 2006;**103**:6332–7.
34. Russo P, Catassi A, Malacarne D, et al. Tumor necrosis factor enhances SN38-mediated apoptosis in mesothelioma cells. *Cancer* 2005;**103**:1503–18.
35. Ozvaran MK, Cao XX, Miller SD, et al. Antisense oligonucleotides directed at the Bcl-xl gene product augment chemotherapy response in mesothelioma. *Mol Cancer Ther* 2004;**3**:545–50.
36. Thomadaki H, Scorilas A, Hindmarsh JT. BCL2 family of apoptosis-related genes: functions and clinical implications in cancer. *Crit Rev Clin Lab Sci* 2006;**43**:1–67.
40. Lewis RJ, Garcia ML. Therapeutic potential of venom peptides. *Nature Rev* 2003;**2**:790–802.
41. Russo P, Pala M, Parodi S, et al. Effects of vitamin E on liver DNA. *Cancer Lett* 1984;**25**:163–70.